

Manufacturing Large-scale Materials with Structural Color

Lukas Schertel^{a§}, Sofia Magkiriadou^{a§}, Pavel Yazhgur^a, and Ahmet F. Demirörs^{*ab}

Abstract: Living organisms frequently use structural color for coloration as an alternative mechanism to chemical pigmentation. Recently there has been a growing interest to translate structural color into synthetic materials as a more durable and less hazardous alternative to conventional pigments. Efforts to fabricate structurally colored materials take place on different fronts, from 3D printing to spray-coating and roll-to-roll casting. Stability, performance, and quality of the color, the environmental impact of the materials or their manufacturing methods are some of the heavily researched topics we discuss. First, we highlight recent examples of large-scale manufacturing technologies to fabricate structurally colored objects. Second, we discuss the current challenges to be tackled to create perfect appearances which aim at the full color gamut while caring for environmental concerns. Finally, we discuss possible scenarios that could be followed in order to involve other manufacturing methods for creating structurally colored objects.

Keywords: Additive manufacturing · Manufacturing methods · Structural color · Sustainability

1. Introduction

Color is an important aspect of everyday life, both for aesthetic reasons, for example in art and design, as well as for information transfer, for example in sensory systems or for traffic regulation. Color usually originates from pigmentary absorption, where an organic molecule or transition metal ion absorbs light wavelength-dependently due to its interactions with the electronic structure. Another mechanism to create coloration is through scattering from structured materials, where interference of light scattered by a periodic nanostructure whose period is comparable in size to the wavelengths of light, causes color. Today pigmentary coloration is still the main way of coloration, although it has raised several environmental concerns. It is known that many pigments cause pollution starting from their production, during their applications and after they have been used, for instance they cause health hazards when digested by humans or animals.^[1] One other disadvantage of pigmentary coloration is their photo- or thermal-instability. When exposed to light or heat, pigments made from organic molecules tend to degrade and bleach. Similarly, inorganic pigments, usually containing hazardous heavy transition metal atoms, may also run into oxidation and color fading issues *e.g.* when they are exposed to heat.^[2] Therefore, creating color without the use of absorbing dyes and pigments is of interest, in order to circumvent health and safety hazards as well as solve stability issues.

Nature has created excellent examples of structural coloration where photobleaching-resistant and stable color can be achieved and controlled without the use of pigments. Periodic nanostructures in the forms of multilayers, 2D arrays of scattering objects, or photonic crystals can be found in iridescent gemstones called opals^[3–5] as well as in butterfly wings,^[6] beetles^[7] and fish.^[8,9] Color in some of the above-mentioned natural photonic materials depends on the illumination angle and observation, which leads to the characteristic iridescence. Iridescence limits the suitability of structural color as an alternative to isotropic coloration generated by absorption-based pigments. Therefore, creation of angle-independent structural color is on the radar of scientists. The angle

dependency of the color is related to the order of the scattering units in the structure and their arrangement, and researchers have recently shown that isotropic structural colors can be obtained by creating disordered scattering systems.^[10–12] Because structural color is based on interference of scattered light, the color depends on a few material parameters such as the refractive index of the scatterers and its contrast to the continuum refractive index, the solid fraction of scatterers and the length scale of the periodicity of the structure. Note that structural coloration does not explicitly depend on the exact chemistry of the materials but rather on the material physical properties. This is indeed advantageous for materials selection in designing structural color because the same color appearance can be achieved by a variety of materials. Such an advantage turns out to be critical, especially for picking sustainable and bio-sourced material options for alternative coloration strategies of the future, which constitutes one of the main motivations of the current interest in structural color research.

Some of the many ways of synthetically creating structural color can be listed as nanofabrication of metasurfaces, self-assembly of colloids or block co-polymers and multi-layer film fabrication.^[13–15] Because structural color requires periodic materials with features at a length scale that is similar to the wavelength of visible light, *i.e.* on the order of a few hundred nanometers, assembly of building blocks which are already at this length scale simplifies the fabrication process. Therefore, out of these strategies, colloidal self-assembly distinguishes itself to be prominent for its promises in relatively simple production, scalability and possibility of creating 3D bulk structures. Whereas, top-down approaches that achieve such resolution are often constrained to 2D.

Consequently, colloidal self-assembly has been intensively used to prepare and understand structural color from many aspects.^[16–18] Colloidal self-assembly often employs colloidal nanoparticles as the building blocks and assembles them in a bottom-up fabrication fashion. However, many manufacturing techniques used in industry today require a top-down approach where a known bulk shape is given to a material that is continuously fed

*Correspondence: Dr. A. F. Demirörs, E-mail: ahmet.demiroers@unifr.ch

^aDepartment of Physics, University of Fribourg, CH-1700 Fribourg, Switzerland; ^bComplex Materials, Department of Materials, ETH Zurich, CH-8093, Zurich, Switzerland

[§]Equal contribution

to the fabrication setup. To date, the use of bulk material fabrication methods to create objects with structural color applications is rare.^[19–21] To obtain objects with particular design and shape which are colored with alternative structural coloration strategies, current manufacturing technologies have to be combined with self-assembly routes for structural color. This primarily requires the combination of the top-down approach of the fabrication methods with the bottom-up approach of the self-assembly which gives rise to the structural color.

Here we first discuss the already reported examples that combine current manufacturing technologies with structural coloration routes *via* self-assembly. Second, we discuss the current challenges to be tackled to create perfect alternatives for the coloration of the future which aims at the full-color gamut while caring for environmental concerns. Finally, we discuss possible scenarios that could be followed in order to involve other manufacturing methods for creating structurally colored objects.

It is worth noting here that many coloration applications do not always require bulk color, but rather a surface coating of single or multiple colors. Therefore, we will also discuss manufacturing methods for surface applications such as spraying and ink-jet printing. It is also worth mentioning that such surface coating methods require development of new methods to incorporate structural color pigments in paints, coatings and inks.

2. Manufacturing Colored Objects

2.1 State of the Art

There has been significant interest in reproducing structural color synthetically and this has motivated scientists to use various methods to produce structurally colored films/coatings^[22] and also pigments using colloidal assembly. These methods include colloidal assembly by using microfabricated templates,^[14] external fields^[23,24] or deposition techniques for coatings^[22] and include microfluidic encapsulation and fabrication of supra-structures from polymers,^[25] liquid crystals^[26] and colloids.^[27] Most of these demonstrations aimed for the production of the color, the colored surface or pigment particles and did not focus on the production of large-scale materials with color. Recently scientists have started to take this into account and shown promising examples that combined manufacturing methods with structural color that originates from colloidal self-assembly.

Pressing is a commonly used method for industrial production and recently Takeoka and co-workers used this method to produce disc-like structures with color^[21] (Fig. 1A and 1B). Here they assembled monodisperse silica nanoparticles and mixed them with carbon black to achieve color saturation. Pressing was used for compaction of the powder and resulted in color after reaching a solid volume fraction of $\sim 50\%$. Pressing also increased the mechanical strength of the particle assembly and gave the final shape of the colored object. Although the pressing technique has possibilities to obtain simple shapes other than discs *via* shaping the pressing bed, here the shape was limited to discs. In addition, the

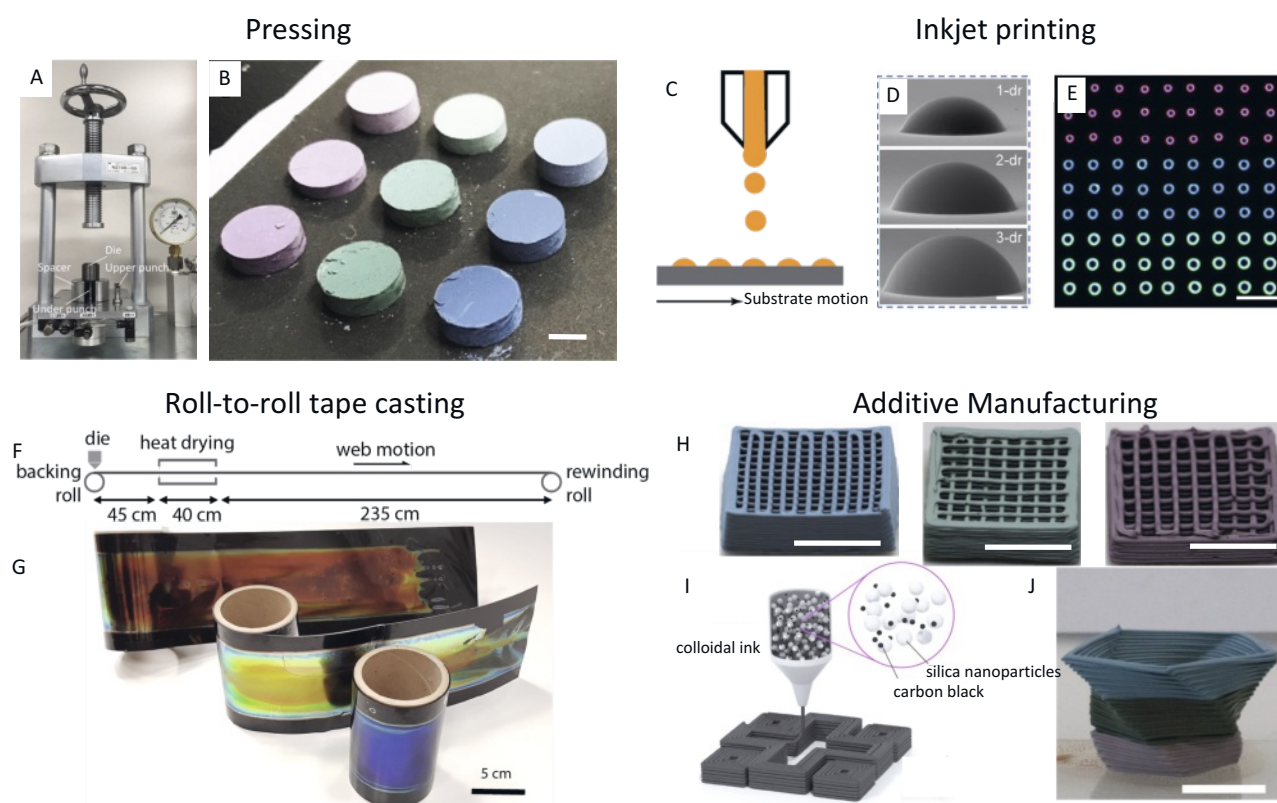


Fig. 1. Large-scale fabrication and shaping of bulk structurally colored assemblies. A) Pressing tool used to press powders into pellets. B) Samples pressed from silica nanoparticles with varying particle sizes and carbon black concentrations. Scale bar 1 cm. Panels A & B adapted with permission from ref. [21]. Copyright 2019 American Chemical Society. C) Sketch of the setup which depicts the working principle of inkjet printing. D) Deposited droplets of silica nanoparticles for achieving structural color with different droplet sizes for controllable printing resolution. Adapted with permission from ref. [28]. Copyright 2021 American Chemical Society. E) An example of inkjet printing of vivid colors with different colors and sizes created from liquid crystal forming polymer brushes. Scale bar 100 μm . Adapted from ref. [29]. F) Sketch showing the roll-to-roll (R2R) casting setup. G) Examples of casted macroscopic samples with structurally colored thin films. Red, green and blue R2R-cast CNC films deposited onto a black PET web. Images are courtesy of Benjamin Drouget and Silvia Vignolini. H) 3D printed objects with the direct write method. The printed grid structures were created with a silica nanoparticle ink that contains carbon black. The size of the nanoparticles increases from 200 to 300 nm from left to right. Scale bar 1 cm. I) Sketch that shows the direct write printing setup with the ink ingredients. J) A multicolor vase demonstrating the possibility of printing complex objects with spatial and temporal control with multiple colors. Scale bar 1 cm. Panels H–J are adapted from ref. [34].

final pressed object was not robust enough to further process for shaping purposes.

When it comes to surface coloration, ink-jet printing is a possible method of choice. Ink-jet printing sprays relatively monodisperse droplets on flat or curved surfaces which, upon evaporation, solidifies and forms programmable patterns with high resolution. Recently this method was applied to form well-controlled and colored patterns with structural coloration.^[28,29] One of the methods used the assembly of colloidal particles^[28] (Fig. 1C and 1D) and another one used the assembly of polymer brushes^[29] for vivid colors (Fig. 1E). The usual approach consists of jetting a nanoparticle dispersion and consecutively drying it directly on a substrate. Special attention should be paid to avoid nozzle clogging and the coffee-ring effect after drying. Depending on substrate properties, different morphologies can be achieved, such as mono- and multilayers or microdome aggregates.^[30] This approach, however, severely limits the range of available substrates and complicates color mixing. The potential solutions are to dry dispersions in flight^[31] or print pre-assembled colorful colloidal aggregates.^[32,33]

Tape-casting is a method that is used for creating thin films and is usually combined with a roll-to-roll setup for continuous production in industry. A neat example of tape-casting for structurally colored films was shown by Vignolini and co-workers.^[35] They assembled cellulose nanoparticles for structural coloration and created thin films with color continuously (Fig. 1F and 1G). Although the mechanical strength of the film should be enhanced for industrial applications this is a breakthrough in the field, which demands sustainable coloration alternatives.

Additive manufacturing methods have received significant attention due to their strength in shape complexity for relatively low cost. To this end, colloidal assembly and co-polymer assemblies were used to 3D print structural color recently.^[36–39] However, in these examples the colors were angle-dependent due to the ordered nature of the assembled constituents. It has been shown that disordered assemblies of colloidal particles provide angle-independent structural coloration. Recently 3D printing of colloidal particles with isotropic coloration was successful.^[34] Here researchers have shown that silica particles mixed with a co-polymer and carbon black can be optimized to have the right consistency to prepare an ink for extrusion.^[34] Such an ink can be extruded from a nozzle to obtain complex geometries. These complex-shaped particle assemblies were colorful after degradation of the co-polymer which increased the solid packing of the particles. As a result of this increased solid fraction a colloidal glass with isotropic color is observed (Fig. 1H to 1J). Note that the removal of the copolymer here not only increases the solid packing but also increases the refractive index contrast between the assembled particles and the continuous medium. This is because the copolymer has a refractive index which is close to the silica particles, therefore its removal leaves behind air which has a significant contrast with the silica nanospheres, and leads to stronger reflection.

2.2 Structural Color Appearance and its Challenges

While a variety of techniques can be adapted to achieve large-scale materials with structural colors, open challenges remain regarding their final appearance. One drawback of structural color compared to conventional pigments concerns the limited available color gamut, in particular for angle-independent colors. The colors of photonic crystals can cover the visible spectrum, and they often stand out for their brilliance and iridescent appearance. However, iridescence is a strong visual effect that is not always desirable. Moreover, manufacturing crystalline structures over large scales can be challenging. Polycrystalline materials are easier to make, but in that case the appearance can be patchy, as, for instance, in natural opals. By contrast, the colors of disordered photonic materials are non-iridescent, and thus look similar to absorbing dyes. This makes them appealing for a variety of applications, as

underneath their ‘normal’ appearance lie the advantages of structural color outlined above: colorfastness, sustainability, as well as the potential for dynamic tunability. In addition, the fact that these materials are inherently disordered at large scales can facilitate their application, as the tolerance in their structural defects can be higher. However, the available palette of the colors of disordered photonic materials is currently limited: yellow, orange, and red colors have poor color purity.^[40,41] Moreover, achieving optimal color saturation for all colors requires special considerations. The challenges to color purity and saturation arise from several distinct optical phenomena that we outline below.

The creation of pure yellow, orange, or red angle-independent structural colors requires the design of materials that have a scattering peak at long wavelengths. This peak can arise from constructive interference between neighboring scatterers. To achieve a peak in the red, these scatterers have to be further apart compared to those in a material designed to be blue. In such materials, however, there are often other concurrent optical effects that favor the scattering of blue light. One such effect arises in materials made out of close-packed colloidal particles embedded in a medium of lower refractive index, a common approach (see Fig. 1B, 1H, 2A). In these materials the particle diameter sets the average interparticle spacing and thus affects the resonant color. Saturated blue can routinely be achieved with particles about ~150–200 nm in diameter for typical polymeric materials in air.^[12,42] However, simply increasing the particle size does not lead to red structural color (Fig. 2A). This is due to resonances within the individual particles, where they act like cavities and scatter preferentially in the blue. In smaller particles, these resonances are in the UV, therefore invisible to the human eye. However, for particles that are larger than ~250 nm, these resonances enter the blue side of the visible spectrum, mix with red, and yield purple or magenta hues, reducing color purity.^[40,41] This issue can be mitigated by designing materials where these single-particle scattering resonances return to the UV range. One such approach is to create structures out of core-shell particles where the scattering cores are smaller than the inter-particle spacing (Fig. 2B),^[43] and another is to create ‘inverse’ structures, where the particles have a lower refractive index than the surrounding medium (Fig. 2C).^[40,44,45] Of course these two approaches can be combined (Fig. 2D).^[46] Taking inspiration from nature and its impressive palette of vivid colors, it is also possible to mix chemical and structural coloring by adding pigments,^[47] for instance absorbing in blue, however in this case the advantages of structural coloration could be mitigated by the need for a conventional dye.

Special considerations also need to be taken to optimize color saturation for all angle-independent structural colors. Color saturation can be compromised mainly by two effects. The first is related to angle independence itself: materials with angle-independent structural colors are generally isotropic, which is achieved by introducing randomness in their internal structure. This means that the characteristic length scale of structural correlations that gives rise to resonant scattering is not as well defined as it is, for instance, in crystals. Thus, the resulting reflection peaks are also generally wider and lower in amplitude than those of crystalline structures. This tradeoff between angle independence and color saturation is indeed a topic of active investigation.^[48] The second effect that can compromise color saturation is multiple scattering, which leads to a broadband background. This is because multiply scattered light traverses distances inside the material that are longer than the extent of correlations between scattering points. As a result, there is no longer constructive interference to select a specific range of wavelengths, but instead all wavelengths can be reflected back to the viewer. This mixing of wavelengths is less of an issue in photonic crystals. In perfect crystals it simply does not occur, because light at off-resonant wavelengths interferes destructively. In imperfect crystals, multiply scattered light can

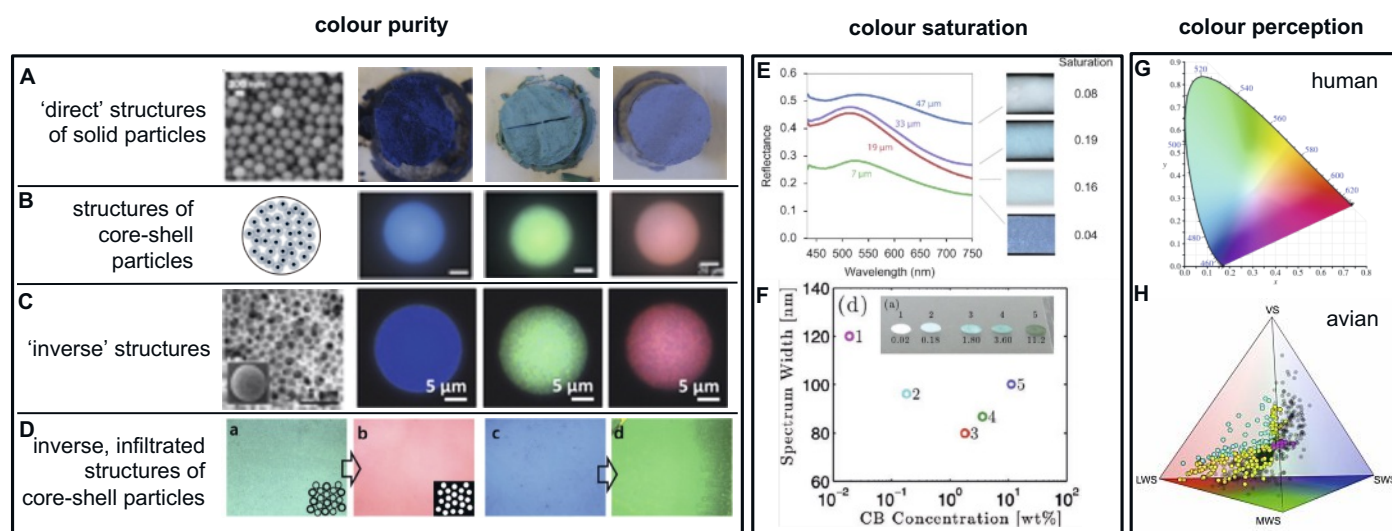


Fig. 2. Structural color appearance and its challenges. A) Black and white image: scanning electron micrograph of a disordered packing of polystyrene spheres. Scale bar is 200 nm. Adapted with permission from ref. [49]. Copyright 2020 American Physical Society. Color images: photographs of disordered packings of poly-methyl-methacrylate particles, mixed with carbon black. These samples are a few mm in size. Particle size increases from left to right. Adapted with permission from ref. [40]. Copyright 2014 American Physical Society. B) Schematic, and micrographs in reflection mode, of photonic balls containing disordered packings of core-shell particles with scattering polystyrene cores and transparent poly(*N*-isopropylacrylamide-*co*-acrylic-acid) shells. Blue, green, and red structural colors are obtained using different shell thicknesses. Scale bar is 20 microns. Adapted with permission from ref. [43]. Copyright 2014, Wiley-VCH. C) Black and white image: cross-sectional scanning electron micrograph of the internal nanoarchitecture of a photonic pigment of the 'inverse' type. The primary material is poly(*n*orbornene-*graft*-polycaprolactone)-*block*-poly(*n*orbornene-*graft*-polyethylene glycol), a biocompatible bottlebrush block copolymer. Color images: optical micrographs of microspheres containing such inverse, porous structures, formed from monodisperse toluene/water microdroplets via controlled evaporation at different temperatures ($T = 22\text{--}80\text{ }^{\circ}\text{C}$). Adapted with permission from ref. [45]. D) Micrographs, in reflection mode, of disordered packings of bidisperse hollow silica particles. The particles used to make the sample shown in panel (a) are larger than the particles used to make the sample shown in panel (c). Panels (b), (d) show the change in color from panels (a), (c), respectively, after infiltration of the packings with trimethylolpropane ethoxylate triacrylate, a photocurable monomer, resulting in a transformation from a 'direct' structure, shown schematically in the inset of panel (a), to an 'inverse' structure, shown schematically in the inset of panel (b). Adapted with permission from ref. [46]. Copyright 2017 American Chemical Society. E) Reflection spectra and dark-field optical micrographs of disordered packings of polystyrene nanospheres with the same sphere diameter but different sample thickness. The calculated value for color saturation is listed on the right. Adapted with permission from ref. [49]. Copyright 2020 American Physical Society. F) Inset: photographs of five drop-cast films of polystyrene spheres containing carbon black. The sample numbers are listed above the samples, and the corresponding wt% of carbon black is listed below. Main graph: the width of the spectra of the reflection peak for each sample. Adapted with permission from ref. [12]. Copyright 2010, Wiley-VCH. G) The CIE 1931 color space chromaticity diagram, one of the standards used to represent color space. Adapted from Wikipedia.^[56] H) The avian four-dimensional color space, where the black points represent the gamut of all avian plumage colors. Reproduced with permission from ref. [57]. Copyright 2022, National Academy of Sciences, U.S.A.

evade destructive interference, for instance due to defects or due to the finite size of the material; still, it is less pronounced than in disordered photonic materials, where the spatial correlations are short-ranged only. In disordered materials, multiple scattering can be mitigated by carefully controlling the sample thickness (Fig. 2E)^[49] or by adding broadband absorbers, such as carbon black (Fig. 2F)^[12,47,50] to limit the sample's optical thickness. Since samples that are too thin tend to be transparent, while samples that are too thick tend to be white, there is typically an optimal thickness that can be calculated depending on the materials involved.^[49]

A few other effects have been identified as potential obstacles to color saturation in amorphous photonic materials. Even before the onset of multiple scattering, scattering processes of a few events can also contribute to the final color. For instance, in the inverse structures of bird feathers double scattering has been shown to generate a secondary reflection peak,^[51] while in colloidal photonic glasses a similar peak has been attributed to light that undergoes total internal reflection at the sample-air interface before scattering again and exiting the sample.^[49] Last but not least, when it comes to fine-tuning color, it needs to be noted that the shape of the reflection spectra can be affected by other parameters such as surface roughness or wavelength-dependent absorption naturally present in the ingredients.^[52]

For practical applications it is important to compartmentalize structurally colored materials in the form of colorful microobjects, thus they stay compatible with industrial techniques using

chemical pigments. A popular approach to achieve this goal is to use spherical aggregates of nanoparticles – 'photonic balls'.^[27] The spherical symmetry of photonic balls ensures particularly low angle dependency and homogeneous color. The colorful nature of individual photonic balls can potentially simplify color mixing. The films of photonic balls, however, strongly suffer from multiple scattering, which arises not only from internal multiple scattering inside photonic balls but also scattering between distinct photonic balls. Thus, such photonic ball films suffer either from strong white appearance or low brightness if high enough concentrations of black absorber are used. These drawbacks can be potentially overcome by changing the photonic ball structure, such as using inverse structures or core-shell particles.

Finally, to close the gap between research and application it is essential to understand the optical phenomena that come into play in the context of the environment in which these colors would be used. Several factors are important in this context. One is the type of illumination, and in particular whether it is directional or diffuse. The structural colors of photonic glasses are truly angle-independent under diffuse illumination, *i.e.* when light arrives from many different directions; however they still show some weak dependence on the viewing angle when illumination is directional.^[12,40,51,53] Still, this angular dependence is typically weaker than in photonic crystals.^[11] Last but not least, the reflection spectra of structural colors are of limited practical use unless they are related to color perception, *i.e.* the color seen by an observer in

response to the reflected light. To underline this, we note here an interesting fact from the avian world. Birds have achieved an impressive range of colors, thanks to pigments as well as structural coloration. To us, human observers, they are one of the most colorful species on our planet. Yet the range of colors they can achieve in their plumage is only a small subset of the color gamut they can see with their tetrachromatic vision (Fig. 2G, H).^[54] The importance of relating the optical response to color quality has been increasingly appreciated by the structural color community in recent years, and color standards are now often used in order to complement the characterization of the reflection spectra of photonic materials in the literature.^[32,41,44,45,50,52,55]

The challenges of the visual appearance of angle-independent structural color should not discourage the development of techniques for their mass production. In a historical coincidence, let us remember that the color blue has also played an important role in the development of photography: one of the first photographic techniques was the cyanotype, a method for imprinting images in shades of blue still used today in art. If we continue to develop ways to apply structural color on the large scale using the colors currently available, we will be ready to extend them to the full palette once this has been achieved.

2.3 Sustainability

Manufacturing color into large-scale applications comes with the challenge of availability and cost efficiency of the raw material. Commercially available color pigments and dyes can be very cost effective but are nowadays often heavy-metal based, made from toxic molecules or by plastic polluting polymeric resources. A sustainable choice of the building blocks for artificially made objects, including color pigments, is essential from a health safety as well as an environmental aspect.^[58,59]

The possibility to create colored objects through scattering by structured materials instead of absorbing dyes increases chances for the choice of sustainable building blocks.

One example is block copolymers (BCPs), that have drawn recent attention by achieving a wide palette of angular independent structural color through designing inverse photonic ball structures.^[45] However, there is an urgent need to consider their environmental impact (microplastic pollution). Progress has been made by showing the full range of colors can be reached using biocompatible bottlebrush block copolymers (BBCPs).^[13]

In this context, nature can serve as a primary example. Inherently the colors created by natural organisms use biocompatible and renewable materials.^[60,61] Structural color in nature is used to achieve stunning appearances from shimmering gold^[62] to matt blue^[41] and bright white.^[63]

The majority of biological materials are based on just a few substances – proteins (e.g. silk), polysaccharides (such as chitin and cellulose) and a few minerals (Fig. 3A–D and F).^[64] While these have poorer basic properties (such as a low refractive index) than engineered materials, nature achieves a wide range of appearances by assembling them into a diversity of structures. Additionally we can learn from natural structures how hierarchical assembly allows us to achieve multifunctionality. As an example, surface nanostructures can combine light manipulation with mechanical protection or water repellency^[65] and chitin in insects and arthropods is often used to build carapaces and sensory systems.

Often building blocks extracted from biological resources are used to build biocompatible non-toxic structurally colored systems. Chitin nanocrystals (ChNCs) can be isolated from two phylogenetically distinct sources of α -chitin, namely mushrooms and shrimps, to achieve structurally colored films^[66] (Fig. 3A). Although it is possible to achieve helicoidal architectures, inspired by structural coloration in arthropods, through exploiting the self-assembly of chitin nanocrystals (ChNCs), structural col-

oration has just been achieved with the same material very recently^[66] and awaits to be tested at a larger scale.

Another example is silk-based photonic materials used to achieve a wide range of structural colors and optical appearances by combining templated self-assembly and nanosurface engineering by heat and UV sensitivity of silk proteins.^[67,68] Most silk utilized in scientific, medical, and commercial endeavors is derived from cocoons of *B. mori* domestic silk moths. Silk cocoons are first degummed (e.g. through a boiling process), then dissolved in a concentrated salt solution followed by a washing step (e.g. dialysis) to obtain an aqueous solution (Fig. 3C). In an annealing/post processing step the photonic structured material can be obtained. As a structural protein, silk fibroin undergoes a conformational transition among β -sheets, random coils, and helices upon exposure to external stimuli, such as water vapor, methanol, and deep UV light allowing to tune the structural properties on the nanoscale obtaining photonic crystal structures (Fig. 3G), diffraction gratings and transparent films whose appearance can be dynamically tuned.

Cellulose is particularly advantageous for the manufacture of sustainable products because of its abundance as the most widely available biopolymer on earth, and its intrinsic renewability aspect.^[69] Cellulose, as the major component of the plant cell wall, is abundant in a hierarchical fibrillar form, which consists of microfibrils that are composed of microfibrils (Fig. 3B). Macroscopic cellulose fibers are widely used in papermaking and the production of cellulose-based polymers.^[70] Recent progress in extraction of nanocellulosic components enables the use for high-tech applications due to the unique chemical and physical properties of cellulose at the nano-scale. For photonic pigments and coatings, cellulose high refractive index and birefringence compared to other biopolymers^[71] enable strong color saturation and thin film applications.^[72]

Nanocelluloses can be classified into two categories based on their dimensions: cellulose nanofibrils (CNFs)^[73] and cellulose nanocrystals (CNCs).^[74]

The intrinsic high value of anisotropy of cellulose fibrils in terms of refractive index and aspect ratios also makes them well suited for highly scattering materials. The optical properties of membranes composed of CNFs can achieve highly bright white,^[75] even in thin coatings. Recently a new class of cellulose particles (CMP) in the micron range has been explored as scattering enhancers.^[76] This is extremely relevant for industrial applications as commercially available white products, such as paints, inks and coatings, are typically formulated with high-refractive-index nanoparticles, for example TiO_2 , as scattering enhancers, which have recently raised serious health and environmental concerns.^[77–79]

Most effort has however been made in developing CNC-based optically structural color pigments and films. The long time known cholesteric liquid-crystalline behavior in suspension^[80] only recently has been transformed into structural color manufacturing in the form of films^[35] and pigments^[72,81] (Fig. 3E). In analogy to liquid-crystal molecules, these rod-like colloids spontaneously form, above a critical concentration, a chiral nematic structure whereby individual CNCs align along a helicoidally birefringent superstructure. This organization gives rise to structural color, strongly depending on the orientation of the cholesteric domains and the pitch length in the structure, thus being very sensitive to assembly conditions as well as mechanical deformations and the chemical environment. While such sensitivity can be a challenge for large scale manufacturing it also offers opportunities for applications. As an example, cellulose derivatives have been used to obtain structurally colored coatings, and found application as low-cost and scalable mechano-chromic pressure sensors,^[82] compatible with roll to roll manufacturing.^[35]

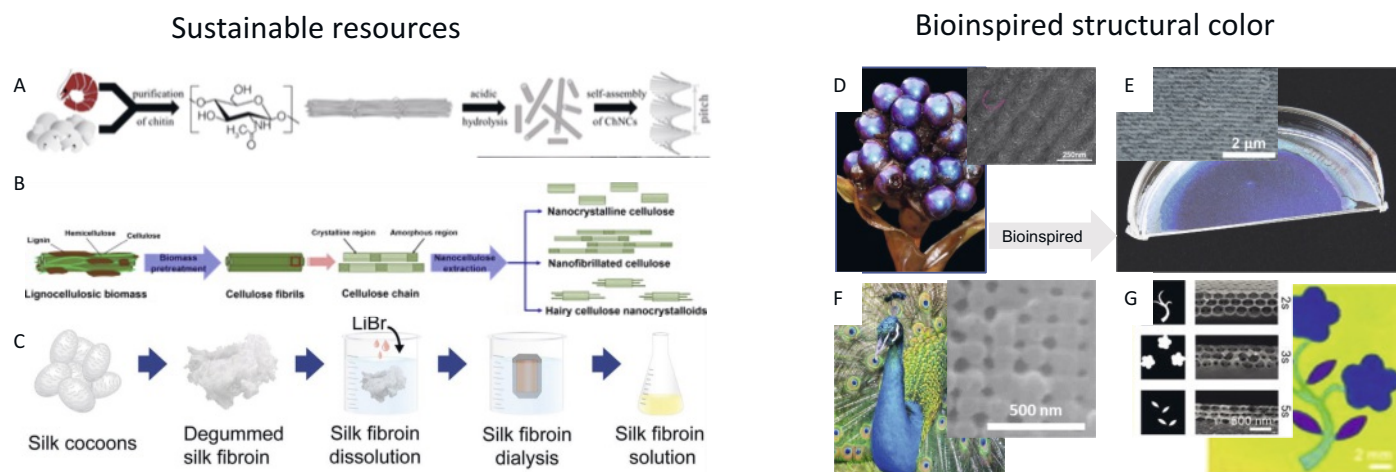


Fig. 3. Sustainable and bioinspired structural color materials. A) Schematic of the extraction process of chitin nanocrystals and their assembly to helicoidal structures as the basic unit for structural color creation through helicoidal self-assembly. Reproduced with permission from ref. [66]. Copyright 2022, Wiley-VCH. B) Schematic of the extraction process of cellulose nanocrystals and their assembly to helicoidal structures. Reproduced from ref. [84]. C) Extraction and processing diagram of silk cocoons into silk fibroin solution as a natural material for photonic structures. Reproduced with permission from ref. [68]. Copyright 2022, Walter de Gruyter. D) Image of the *Pollia condensata* fruit. Inset: SEM Image of the helicoidal cellulose structure found in the fruit's cell wall as the origin for the blue color. Reproduced with permission from ref. [61]. Copyright 2022, National Academy of Sciences, U.S.A. E) Bioinspired cellulose nanocrystal film showing blue structural color. Reproduced with permission from ref. [85]. Copyright 2022, Wiley-VCH. Inset: Image of CNC layers in cross-section SEM. Reproduced with permission from ref. [86]. Copyright 2022, Wiley-VCH. F) Peacock showing its full palette of (structural) color (unsplash free license). Inset: SEM image of the crystalline structure found in peacock feathers. Reproduced with permission from ref. [87]. Copyright (2003) National Academy of Sciences, U.S.A. G) Picture painted by templating silk fibroin solution into a photonic crystal structure,^[88] Copyright 2022, Wiley-VCH.

Further methods from 3D printing of structurally colored cellulose derivative assemblies^[26] to nanoscale patterning for color creation *via* focused electron-beam-induced conversion^[83] have proven the wide range of manufacturing potential for structurally colored cellulose-based materials.

2.4 Towards Multifunctional Materials

When successful fabrication of objects with structural color and shape complexity is achieved, the next challenge will be aiming for the manufacture of multifunctional materials with desired, programmable properties. Possible complementary functions can be programming the surface wetting properties or improving the mechanical, thermal, light durability of these objects.

Wettability: To make complex objects with color and with superhydrophobic surfaces for instance, one can use colloidal building blocks which are superhydrophobic in the first place. When these nanoparticles have the dimensions of the colloids used for obtaining structural color, these assemblies can aim for superhydrophobic structurally colored objects. We envision that the raspberry-shaped superhydrophobic particles like the ones made by D'Acunzi *et al.*^[89] can be used in order to self-assemble multifunctional 3D printed objects which combine complex shape, structural coloration with surface superhydrophobicity.

Mechanical strength: Since the objects are assembled from nanocolloids, the mechanics of the assembled structures for structurally colored objects are usually limited and depend solely on van der Waals forces between the assembled particles. The mechanical strength of silica colloids assembled *via* 3D printing in recent work^[34] had compression strengths up to 8 MPa which is comparable to blackboard chalks. One way to improve the mechanical strength of the assembly is to induce inter-particle chemical bonding between particles after the assembly is achieved. However, such chemical bonding requires modification of the surface chemistry of the colloids and may complicate the upscaling of the used particles. Another strategy to increase the mechanics can be the creation of core-shell colloids with different melting temperatures where the melting temperature, T_{m_core} of

the core, has to be higher than that of the shell, T_{m_shell} . When the temperature T is set to a value between the $T_{m_shell} < T < T_{m_core}$ then the shell will melt and fuse while the core is expected to maintain the order and the structural color. Although there are challenges, such that the pores between the particles can be reduced or the refractive index difference between the core and shell may not be sufficient for coloration, these challenges can be addressed by synthetic chemists to arrive at a product with color and shape-freedom while being capable to withstand thermal and mechanical impacts.

Light and thermal durability: Structural color is considered to be light and thermally durable as long as the periodic nanostructure is maintained. However, when carbon black is used to enhance the color saturation, this light and thermal durability is lowered because of the possible degradation of carbon black under such conditions. Note that researchers^[34] have reported thermal stability up to 1000 °C but these experiments were performed in Ar atmosphere which avoided the degradation of carbon at elevated temperatures. A logical step to avoid this lower stability would be the use of broadband absorbers of oxides which could stand higher temperatures. This was indeed recently demonstrated by Yamanaka *et al.*^[90] who showed stable structurally colored samples up to a temperature of 900 °C in air.

3. What Other Manufacturing Technologies Can Be Used?

3.1 Pressing

In industry pressing combined with machining is used heavily for creating shaped ceramic objects. Pressing is an effective and fast method to make objects with simple shapes templated by the dye or the pressing cavity. Pressed objects usually have disc- or cylinder-like geometries. To make complex geometries the pressed object is then machined and processed. For machining, a binder is usually added to obtain a pressed object that is robust enough to handle and machine. Takeoka and co-workers recently demonstrated that pressing can be used to create discs that are

structurally colored. However, they did not attempt to machine these discs to obtain complex geometries with color. It could be indeed relatively straight-forward to strengthen these discs with a binder additive at the initial mixture. The addition of the binder is expected to give the necessary mechanical stability to handle and machine these objects to allow for colored complex shapes. The use of a variety of colloidal nanoparticle sizes for the assembly of the discs can also result in multi-colored objects with complex geometry.

3.2 Spraying or Additive Manufacturing for Painting

Although there are many examples of surface coating applications based on colloidal assembly of structural color^[91–93] examples of spraying for creating color are rare.^[94,95] One important challenge in spraying colloidal particles is the lack of control in the drying of sprayed droplets which usually results in ordered colloidal assemblies and yields angle-dependent color. One strategy to avoid this could be spraying suspensions of pre-assembled colloidal clusters usually referred to as photonic balls. If the photonic balls are made in a disordered fashion as in the case of Yazhgur *et al.*^[32,33] the spraying is expected to result in angle-independent color. Inkjet printing or 3D printing of such photonic balls or inverse photonic balls can also be a strategy to manufacture objects with color.^[32] Similar to inkjet printing, 3D printing devices can also be used for creating coatings on the surfaces of objects manufactured by other means.^[96] In addition to direct writing of colored inks, additive manufacture of structural color can also be made *via* stereolithography printing,^[97] which is not yet shown and is a more promising printing method for high throughput purposes.

4. Conclusions

Considering the potential advantages of structural color from color stability to sustainability and environmental fronts, the above-mentioned challenges highlight the areas where further development of techniques for mass production of objects with structural coloration is necessary and crucial. Development on the different fronts of the constituents of structural coloration will improve the spectrum of possible applications of future manufacturing methods and thus pave the road to replace pigment dyes with structurally colored alternatives to create color-finished materials.

Acknowledgements

We thank Prof. André Studart (ETH Zurich) and Prof. Frank Scheffold (University of Fribourg) for fruitful discussions and for support. This work was supported by ETH Zürich and the Swiss National Science Foundation through the National Center of Competence in Research Bio-Inspired Materials (grant number: 51NF40_182881).

Received: September 5, 2022

- [1] A. Gürses, M. Açıkyıldız, K. Güneş, M. S. Gürses, 'Dyes and Pigments', Springer International Publishing, **2016**, <https://doi.org/10.1007/978-3-319-33892-7>.
- [2] B. Villmann, C. Weickhardt, *Stud. Conserv.* **2021**, *66*, 167, <https://doi.org/10.1080/00393630.2020.1762401>.
- [3] R. K. Iler, *Nature* **1965**, *207*, 472, <https://doi.org/10.1038/207472a0>.
- [4] Y. Zhao, Z. Xie, H. Gu, L. Jin, X. Zhao, B. Wang, Z. Gu, *NPG Asia Mater.* **2012**, *4*, e25, <https://doi.org/10.1038/am.2012.46>.
- [5] F. Marlow, P. Sharifi, R. Brinkmann, C. Mendive, *Angew. Chem. Int. Ed.* **2009**, *48*, 6212, <https://doi.org/10.1002/anie.200900210>.
- [6] S. Kinoshita, 'Structural Colors in the Realm of Nature', World Scientific, **2008**.
- [7] V. Sharma, M. Crne, J. O. Park, M. Srinivasarao, *Science* **2009**, *325*, 449, <https://doi.org/10.1126/science.1172051>.
- [8] D. Gur, B. A. Palmer, B. Leshem, D. Oron, P. Fratzl, S. Weiner, L. Addadi, *Angew. Chem. Int. Ed.* **2015**, *54*, 12426, <https://doi.org/10.1002/anie.201502268>.
- [9] A. R. Parker, *J. Opt. Pure Appl. Opt.* **2000**, *2*, R15, <https://doi.org/10.1088/1464-4258/2/6/201>.
- [10] Y. Takeoka, M. Honda, T. Seki, M. Ishii, H. Nakamura, *ACS Appl. Mater. Interfaces* **2009**, *1*, 982, <https://doi.org/10.1021/am900074v>.
- [11] M. Harun-Ur-Rashid, A. Bin Imran, T. Seki, M. Ishii, H. Nakamura, Y. Takeoka, *ChemPhysChem* **2010**, *11*, 579, <https://doi.org/10.1002/cphc.200900869>.
- [12] J. D. Forster, H. Noh, S. F. Liew, V. Saranathan, C. F. Schreck, L. Yang, J.-G. Park, R. O. Prum, S. G. J. Mochrie, C. S. O'Hern, H. Cao, E. R. Dufresne, *Adv. Mater.* **2010**, *22*, 2939, <https://doi.org/10.1002/adma.200903693>.
- [13] Z. Wang, C. L. C. Chan, T. H. Zhao, R. M. Parker, S. Vignolini, *Adv. Opt. Mater.* **2021**, *9*, 2100519, <https://doi.org/10.1002/adom.202100519>.
- [14] Z. Xuan, J. Li, Q. Liu, F. Yi, S. Wang, W. Lu, *The Innovation* **2021**, *2*, 100081, <https://doi.org/10.1016/j.xinn.2021.100081>.
- [15] R. Riedler, C. Pesme, J. Druzik, M. Gleeson, E. Pearlstein, *J. Am. Inst. Conserv.* **2014**, *53*, 44, <https://doi.org/10.1179/1945233013Y.0000000020>.
- [16] P. Liu, L. Bai, J. Yang, H. Gu, Q. Zhong, Z. Xie, Z. Gu, *Nanoscale Adv.* **2019**, *1*, 1672, <https://doi.org/10.1039/C8NA00328A>.
- [17] K. Li, C. Li, H. Li, M. Li, Y. Song, *iScience* **2021**, *24*, 102121, <https://doi.org/10.1016/j.isci.2021.102121>.
- [18] G. Shang, M. Eich, A. Petrov, *APL Photonics* **2020**, *5*, 060901, <https://doi.org/10.1063/5.0006203>.
- [19] O. L. J. Pursiainen, J. J. Baumberg, H. Winkler, B. Viel, P. Spahn, T. Ruhl, *Opt. Express* **2007**, *15*, 9553, <https://doi.org/10.1364/OE.15.009553>.
- [20] M. Huang, S.-G. Lu, Y. Ren, J. Liang, X. Lin, X. Wang, *J. Text. Inst.* **2020**, *111*, 756, <https://doi.org/10.1080/00405000.2019.1663623>.
- [21] Y. Naoi, T. Seki, R. Ohnuki, S. Yoshioka, Y. Takeoka, *Langmuir* **2019**, *35*, 13983, <https://doi.org/10.1021/acs.langmuir.9b02622>.
- [22] K. Katagiri, Y. Tanaka, K. Uemura, K. Inumaru, T. Seki, Y. Takeoka, *NPG Asia Mater.* **2017**, *9*, e355, <https://doi.org/10.1038/am.2017.13>.
- [23] L. He, M. Wang, J. Ge, Y. Yin, *Acc. Chem. Res.* **2012**, *45*, 1431, <https://doi.org/10.1021/ar200276t>.
- [24] A. C. Arsenault, D. P. Puzzo, I. Manners, G. A. Ozin, *Nat. Photonics* **2007**, *1*, 468, <https://doi.org/10.1038/nphoton.2007.140>.
- [25] Q. Guo, R. Xue, J. Zhao, Y. Zhang, G. T. van de Kerkhof, K. Zhang, Y. Li, S. Vignolini, D.-P. Song, *Angew. Chem. Int. Ed.* **2022**, *61*, e202206723, <https://doi.org/10.1002/anie.202206723>.
- [26] C. L. C. Chan, I. M. Lei, G. T. van de Kerkhof, R. M. Parker, K. D. Richards, R. C. Evans, Y. Y. S. Huang, S. Vignolini, *Adv. Funct. Mater.* **2022**, *32*, 2108566, <https://doi.org/10.1002/adfm.202108566>.
- [27] N. Vogel, S. Utech, G. T. England, T. Shirman, K. R. Phillips, N. Koay, I. B. Burgess, M. Kolle, D. A. Weitz, J. Aizenberg, *Proc. Natl. Acad. Sci. USA* **2015**, *112*, 10845, <https://doi.org/10.1073/pnas.1506272112>.
- [28] Z. Hu, N. P. Bradshaw, B. Vanthournout, C. Forman, K. Gnanasekaran, M. P. Thompson, P. Smeets, A. Dhinojwala, M. D. Shawkey, M. C. Hersam, N. C. Gianneschi, *Chem. Mater.* **2021**, *33*, 6433, <https://doi.org/10.1021/acs.chemmater.1c01719>.
- [29] K. Li, T. Li, T. Zhang, H. Li, A. Li, Z. Li, X. Lai, X. Hou, Y. Wang, L. Shi, M. Li, Y. Song, *Sci. Adv.* **2021**, *7*, eabh1992, <https://doi.org/10.1126/sciadv.abh1992>.
- [30] J. Zhang, Z. Zhu, Z. Yu, L. Ling, C.-F. Wang, S. Chen, *Mater. Horiz.* **2019**, *6*, 90, <https://doi.org/10.1039/C8MH00248G>.
- [31] E. Sowade, T. Blaudeck, R. B. Baumann, *Cryst. Growth Des.* **2016**, *16*, 1017, <https://doi.org/10.1021/acs.cgd.5b01567>.
- [32] P. Yazhgur, N. Muller, F. Scheffold, *ACS Photonics* **2022**, *9*, 2809, <https://doi.org/10.1021/acsp Photonics.2c00627>.
- [33] P. Yazhgur, G. J. Aubry, L. S. Froufe-Pérez, F. Scheffold, *Opt. Express* **2021**, *29*, 14367, <https://doi.org/10.1364/OE.418735>.
- [34] A. F. Demirörs, E. Poloni, M. Chiesa, F. L. Bargardi, M. R. Binelli, W. Woigk, L. D. C. de Castro, N. Kleger, F. B. Coulter, A. Sicher, H. Galinski, F. Scheffold, A. R. Studart, *Nat. Commun.* **2022**, *13*, 4397, <https://doi.org/10.1038/s41467-022-32060-2>.
- [35] B. E. Droguet, H.-L. Liang, B. Frka-Petesic, R. M. Parker, M. F. L. De Volder, J. J. Baumberg, S. Vignolini, *Nat. Mater.* **2022**, *21*, 352, <https://doi.org/10.1038/s41563-021-01135-8>.
- [36] J. B. Kim, C. Chae, S. H. Han, S. Y. Lee, S.-H. Kim, *Sci. Adv.* **2021**, *7*, eabj8780, <https://doi.org/10.1126/sciadv.abj8780>.
- [37] B. M. Boyle, T. A. French, R. M. Pearson, B. G. McCarthy, G. M. Miyake, *ACS Nano* **2017**, *11*, 3052, <https://doi.org/10.1021/acsnano.7b00032>.
- [38] B. B. Patel, D. J. Walsh, D. H. Kim, J. Kwok, B. Lee, D. Guironnet, Y. Diao, *Sci. Adv.* **2020**, *6*, eaaz7202, <https://doi.org/10.1126/sciadv.aaz7202>.
- [39] Y. Liu, H. Wang, J. Ho, R. C. Ng, R. J. H. Ng, V. H. Hall-Chen, E. H. H. Koay, Z. Dong, H. Liu, C.-W. Qiu, J. R. Greer, J. K. W. Yang, *Nat. Commun.* **2019**, *10*, 4340, <https://doi.org/10.1038/s41467-019-12360-w>.

- [40] S. Magkiriadou, J.-G. Park, Y.-S. Kim, V. N. Manoharan, *Phys. Rev. E* **2014**, *90*, 062302, <https://doi.org/10.1103/PhysRevE.90.062302>.
- [41] G. Jacucci, S. Vignolini, L. Schertel, *Proc. Natl. Acad. Sci.* **2020**, *117*, 23345, <https://doi.org/10.1073/pnas.2010486117>.
- [42] S. Magkiriadou, J.-G. Park, Y.-S. Kim, V. N. Manoharan, *Opt. Mater. Express* **2012**, *2*, 1343, <https://doi.org/10.1364/OME.2.001343>.
- [43] J.-G. Park, S.-H. Kim, S. Magkiriadou, T. M. Choi, Y.-S. Kim, V. N. Manoharan, *Angew. Chem. Int. Ed.* **2014**, *53*, 2899, <https://doi.org/10.1002/anie.201309306>.
- [44] G. Shang, K. P. Furlan, R. Janßen, A. Petrov, M. Eich, M. Eich, *Opt. Mater. Express* **2020**, *28*, 7759, <https://doi.org/10.1364/OE.380488>.
- [45] Z. Wang, C. L. C. Chan, J. S. Haataja, L. Schertel, R. Li, G. T. van de Kerkhof, O. A. Scherman, R. M. Parker, S. Vignolini, *Angew. Chem. Int. Ed.* **2022**, *61*, e202206562, <https://doi.org/10.1002/anie.202206562>.
- [46] S.-H. Kim, S. Magkiriadou, D. K. Rhee, D. S. Lee, P. J. Yoo, V. N. Manoharan, G.-R. Yi, *ACS Appl. Mater. Interfaces* **2017**, *9*, 24155, <https://doi.org/10.1021/acsami.7b02098>.
- [47] T. Sai, B. D. Wilts, A. Sicher, U. Steiner, F. Scheffold, E. R. Dufresne, *CHIMIA* **2019**, *73*, 47, <https://doi.org/10.2533/chimia.2019.47>.
- [48] M. Xiao, A. B. Stephenson, A. Neophytou, V. Hwang, D. Chakrabarti, V. N. Manoharan, *Opt. Express* **2021**, *29*, 21212, <https://doi.org/10.1364/OE.425399>.
- [49] V. Hwang, A. B. Stephenson, S. Magkiriadou, J.-G. Park, V. N. Manoharan, *Phys. Rev. E* **2020**, *101*, 012614, <https://doi.org/10.1103/PhysRevE.101.012614>.
- [50] L. Schertel, L. Siedentop, J.-M. Meijer, P. Keim, C. M. Aegerter, G. J. Aubry, G. Maret, *Adv. Opt. Mater.* **2019**, *7*, 1900442, <https://doi.org/10.1002/adom.201900442>.
- [51] H. Noh, S. F. Liew, V. Saranathan, R. O. Prum, S. G. J. Mochrie, E. R. Dufresne, H. Cao, *Opt. Express* **2010**, *18*, 11942, <https://doi.org/10.1364/OE.18.011942>.
- [52] V. Hwang, A. B. Stephenson, S. Barkley, S. Brandt, M. Xiao, J. Aizenberg, V. N. Manoharan, *Proc. Natl. Acad. Sci. USA* **2021**, *118*, e2015551118, <https://doi.org/10.1073/pnas.2015551118>.
- [53] D.-P. Song, T. H. Zhao, G. Guidetti, S. Vignolini, R. M. Parker, *ACS Nano* **2019**, *13*, 1764, <https://doi.org/10.1021/acsnano.8b07845>.
- [54] M. C. Stoddard, R. O. Prum, *Behav. Ecol.* **2011**, *22*, 1042, <https://doi.org/10.1093/beheco/arr088>.
- [55] S. Magkiriadou, PhD Thesis Harvard University, No 14226099, **2015**. <http://nrs.harvard.edu/urn-3:HUL.InstRepos:14226099>
- [56] CIE 1931 color space, Wikipedia, cessed 20 Sept. 2022, https://en.wikipedia.org/wiki/CIE_1931_color_space, a.
- [57] M. C. Stoddard, H. N. Eyster, B. G. Hogan, D. H. Morris, E. R. Soucy, D. W. Inouye, *Proc. Natl. Acad. Sci. USA* **2020**, *117*, 15112, <https://doi.org/10.1073/pnas.1919377117>.
- [58] K. L. Law, R. C. Thompson, *Science* **2014**, *345*, 144, <https://doi.org/10.1126/science.1254065>.
- [59] M. A. Browne, P. Crump, S. J. Niven, E. Teuten, A. Tonkin, T. Galloway, R. Thompson, *Environ. Sci. Technol.* **2011**, *45*, 9175, <https://doi.org/10.1021/es201811s>.
- [60] M. Mitov, *Soft Matter* **2017**, *13*, 4176, <https://doi.org/10.1039/C7SM00384F>.
- [61] S. Vignolini, P. J. Rudall, A. V. Rowland, A. Reed, E. Moyroud, R. B. Faden, J. J. Baumberg, B. J. Glover, U. Steiner, *Proc. Natl. Acad. Sci. USA* **2012**, *109*, 15712, <https://doi.org/10.1073/pnas.1210105109>.
- [62] A. E. Seago, P. Brady, J.-P. Vigneron, T. D. Schultz, *J. R. Soc. Interface* **2009**, *6*, S165, <https://doi.org/10.1098/rsif.2008.0354.focus>.
- [63] B. D. Wilts, X. Sheng, M. Holler, A. Diaz, M. Guizar-Sicarios, J. Raabe, R. Hoppe, S.-H. Liu, R. Langford, O. D. Onelli, D. Chen, S. Torquato, U. Steiner, C. G. Schroer, S. Vignolini, A. Sepe, *Adv. Mater.* **2018**, *30*, 1702057, <https://doi.org/10.1002/adma.201702057>.
- [64] M. Eder, S. Amini, P. Fratzl, *Science* **2018**, *362*, 543, <https://doi.org/10.1126/science.aat8297>.
- [65] R. H. Siddique, G. Gomard, H. Hölscher, *Nat. Commun.* **2015**, *6*, 6909, <https://doi.org/10.1038/ncomms7909>.
- [66] A. Narkevicius, R. M. Parker, J. Ferrer-Orri, T. G. Parton, Z. Lu, G. T. van de Kerkhof, B. Frka-Petesic, S. Vignolini, *Adv. Mater.* **2022**, *34*, 2203300, <https://doi.org/10.1002/adma.202203300>.
- [67] G. Guidetti, L. d'Amone, T. Kim, G. Matzeu, L. Mogas-Soldevila, B. Napier, N. Ostrovsky-Snyder, J. Roshko, E. Ruggeri, F. G. Omenetto, *Appl. Phys. Rev.* **2022**, *9*, 011302, <https://doi.org/10.1063/5.0060344>.
- [68] G. Guidetti, Y. Wang, F. G. Omenetto, *Nanophotonics* **2021**, *10*, 137, <https://doi.org/10.1515/nanoph-2020-0358>.
- [69] B. Frka-Petesic, S. Vignolini, *Nat. Photonics* **2019**, *13*, 365, <https://doi.org/10.1038/s41566-019-0448-9>.
- [70] D. Klemm, B. Heublein, H.-P. Fink, A. Bohn, *Angew. Chem. Int. Ed.* **2005**, *44*, 3358, <https://doi.org/10.1002/anie.200460587>.
- [71] E. Lasseguette, D. Roux, Y. Nishiyama, *Cellulose* **2008**, *15*, 425, <https://doi.org/10.1007/s10570-007-9184-2>.
- [72] H.-L. Liang, M. M. Bay, R. Vadrucchi, C. H. Barty-King, J. Peng, J. J. Baumberg, M. F. L. De Volder, S. Vignolini, *Nat. Commun.* **2018**, *9*, 4632, <https://doi.org/10.1038/s41467-018-07048-6>.
- [73] A. Isogai, T. Saito, H. Fukuzumi, *Nanoscale* **2011**, *3*, 71, <https://doi.org/10.1039/C0NR00583E>.
- [74] Y. Habibi, L. A. Lucia, O. J. Rojas, *Chem. Rev.* **2010**, *110*, 3479, <https://doi.org/10.1021/cr900339w>.
- [75] M. S. Toivonen, O. D. Onelli, G. Jacucci, V. Lovikka, O. J. Rojas, O. Ikkala, S. Vignolini, *Adv. Mater.* **2018**, *30*, 1704050, <https://doi.org/10.1002/adma.201704050>.
- [76] H. Yang, G. Jacucci, L. Schertel, S. Vignolini, *ACS Nano* **2022**, *16*, 7373, <https://doi.org/10.1021/acsnano.1c09198>.
- [77] S. Bettini, E. Boutet-Robinet, C. Cartier, C. Coméra, E. Gaultier, J. Dupuy, N. Naud, S. Taché, P. Grysan, S. Reguer, N. Thieriet, M. Réfrégiers, D. Thiaudière, J.-P. Cravedi, M. Carrière, J.-N. Audinot, F. H. Pierre, L. Guzylack-Piriou, E. Houdeau, *Sci. Rep.* **2017**, *7*, 40373, <https://doi.org/10.1038/srep40373>.
- [78] A. Weir, P. Westerhoff, L. Fabricius, K. Hristovski, N. von Goetz, *Environ. Sci. Technol.* **2012**, *46*, 2242, <https://doi.org/10.1021/es204168d>.
- [79] J. Hou, L. Wang, C. Wang, S. Zhang, H. Liu, S. Li, X. Wang, *J. Environ. Sci.* **2019**, *75*, 40, <https://doi.org/10.1016/j.jes.2018.06.010>.
- [80] J.-F. Revol, H. Bradford, J. Giasson, R. H. Marchessault, D. G. Gray, *Int. J. Biol. Macromol.* **1992**, *14*, 170, [https://doi.org/10.1016/S0141-8130\(05\)80008-X](https://doi.org/10.1016/S0141-8130(05)80008-X).
- [81] R. M. Parker, T. H. Zhao, B. Frka-Petesic, S. Vignolini, *Nat. Commun.* **2022**, *13*, 3378, <https://doi.org/10.1038/s41467-022-31079-9>.
- [82] G. Kamita, B. Frka-Petesic, A. Allard, M. Dargaud, K. King, A. G. Dumanli, S. Vignolini, *Adv. Opt. Mater.* **2016**, *4*, 1950, <https://doi.org/10.1002/adom.201600451>.
- [83] T. Ganner, J. Sattelkow, B. Rumpf, M. Eibinger, D. Reishofer, R. Winkler, B. Nidetzky, S. Spirk, H. Plank, *Sci. Rep.* **2016**, *6*, 32451, <https://doi.org/10.1038/srep32451>.
- [84] P. Phanthong, P. Reubroycharoen, X. Hao, G. Xu, A. Abudula, G. Guan, *Carbon Resour. Convers.* **2018**, *1*, 32, <https://doi.org/10.1016/j.crcon.2018.05.004>.
- [85] A. G. Dumanli, G. Kamita, J. Landman, H. van der Kooij, B. J. Glover, J. J. Baumberg, U. Steiner, S. Vignolini, *Adv. Opt. Mater.* **2014**, *2*, 646, <https://doi.org/10.1002/adom.201400112>.
- [86] B. Frka-Petesic, G. Guidetti, G. Kamita, S. Vignolini, *Adv. Mater.* **2017**, *29*, 1701469, <https://doi.org/10.1002/adma.201701469>.
- [87] J. Zi, X. Yu, Y. Li, X. Hu, C. Xu, X. Wang, X. Liu, R. Fu, *Proc. Natl. Acad. Sci. USA* **2003**, *100*, 12576, <https://doi.org/10.1073/pnas.2133313100>.
- [88] Y. Wang, D. Aurelio, W. Li, P. Tseng, Z. Zheng, M. Li, D. L. Kaplan, M. Liscidini, F. G. Omenetto, *Adv. Mater.* **2017**, *29*, 1702769, <https://doi.org/10.1002/adma.201702769>.
- [89] M. D'Acunzi, L. Mammen, M. Singh, X. Deng, M. Roth, G. K. Auernhammer, H.-J. Butt, D. Vollmer, *Faraday Discuss.* **2010**, *146*, 35, <https://doi.org/10.1039/B925676H>.
- [90] T. Yamanaka, N. Tarutani, K. Katagiri, K. Inumaru, Y. Takeoka, T. Masui, *ACS Appl. Mater. Interfaces* **2022**, *14*, 29324, <https://doi.org/10.1021/acscami.2c08649>.
- [91] D. Yang, W. Luo, Y. Huang, S. Huang, *ACS Omega* **2019**, *4*, 528, <https://doi.org/10.1021/acscomega.8b02987>.
- [92] H. Shen, Q. Liang, L. Song, G. Chen, Y. Pei, L. Wu, X. Zhang, *J. Mater. Sci.* **2020**, *55*, 2353, <https://doi.org/10.1007/s10853-019-04118-y>.
- [93] K. W. Klockars, N. E. Yau, B. L. Tardy, J. Majoinen, T. Kämäräinen, K. Miettunen, E. Boutonnet, M. Borghei, J. Beidler, O. J. Rojas, *Cellulose* **2019**, *26*, 491, <https://doi.org/10.1007/s10570-018-2167-7>.
- [94] Y. Takeoka, S. Yoshioka, A. Takano, S. Arai, K. Nueangnoraj, H. Nishihara, M. Teshima, Y. Ohtsuka, T. Seki, *Angew. Chem.* **2013**, *125*, 7402, <https://doi.org/10.1002/ange.201301321>.
- [95] Q. Zeng, C. Ding, Q. Li, W. Yuan, Y. Peng, J. Hu, K.-Q. Zhang, *RSC Adv.* **2017**, *7*, 8443, <https://doi.org/10.1039/C6RA26526J>.
- [96] F. B. Coulter, A. Ianakiev, *3D Print. Addit. Manuf.* **2015**, *2*, 140, <https://doi.org/10.1089/3dp.2015.0017>.
- [97] M. Regehly, Y. Garmshausen, N. Reuter, N. F. König, E. Israel, D. P. Kelly, C.-Y. Chou, K. Koch, B. Asfari, S. Hecht, *Nature* **2020**, *588*, 620, <https://doi.org/10.1038/s41586-020-3029-7>.

License and Terms



This is an Open Access article under the terms of the Creative Commons Attribution License CC BY 4.0. The material may not be used for commercial purposes.

The license is subject to the CHIMIA terms and conditions: (<https://chimia.ch/chimia/about>).

The definitive version of this article is the electronic one that can be found at <https://doi.org/10.2533/chimia.2022.833>